Supplementary Materials for

Local protein kinase A action proceeds through intact holoenzymes

F. Donelson Smith, Jessica L. Esseltine, Patrick J. Nygren, David Veesler, Dominic P. Byrne, Matthias Vonderach, Ilya Strashnov, Claire E. Eyers, Patrick A. Eyers, Lorene K. Langeberg, John D. Scott

*Corresponding author. Email: scottjdw@uw.edu

Published 23 June 2017, *Science* **356**, 1288 (2017)
DOI: 10.1126/science.aaj1669

This PDF file includes

Materials and Methods

cDNAs, Cloning and Mutagenesis

The FRET biosensor constructs for AKAR4^{NES}, AKAR4^{NLS} and ICUE3 were kindly provided by Dr. Jin Zhang (UC San Diego). The R2C2 PKA fusion construct was cloned using Gibson Assembly of PCR products into pcDNA3. The construct consists of full length mouse RIIα cDNA, a segment encoding a linker peptide (WDPGSGSLEAGCKNFFPRSFTSCGSLEGGSAAA), the full-length mouse PKA-Cα cDNA and an epitope tag (AAALEHHHHHH*). Mutagenesis to introduce the "kinase-dead" or analog-sensitive mutations (Lys507Ala or Met555Ala in the full-length R2C2 polypeptide) was performed using inverse PCR with Phusion polymerase (NEB), followed by phosphorylation and ligation of free ends. All oligonucleotides and geneBlock fragments were purchased from Integrated DNA Technologies. All other molecular biology procedures followed standard protocols.

Cell Culture

U2OS cells were a gift from Dr. Heidi Hehnly (SUNY Upstate) and were tested by DDC Medical with results verified by ATCC STR profiling. HEK293A (ThermoFisher) cells were cultured in DMEM-H plus 10% FBS and penicillin/streptomycin (ThermoFisher). U2OS cells were cultured in DMEM-H containing 20 mM HEPES pH 7.4, 10% FBS and pen/strep. Cells were passaged 2-3 times per week using TrypLE reagent (ThermoFisher). U2OS$^{R2A/R2B/CA}$ stably expressing R2C2 were created by transfection with the appropriate vectors, selection with G418 (400 μg/ml) for 2-3 weeks, expansion and screening for expression by immunoblot.

CRISPR-Cas9 Editing of PKA Subunit Genes

Vectors encoding sgRNAs and SpCas9-2A-GFP were provided by Horizon Discovery (Cambridge, UK). Multiple sgRNA sequences were tested for each gene targeted. A combination of three individual vectors that worked in initial experiments were co-transfected into U2OS cells using TransIt-LT1 (Mirus). The guide sequences used are as follows:
PRKAR2A guide 5: GTACTTCACCCGCCTGCGCG
PRKAR2B guide 4: ACTCCAGCAGGTCCGCGGGC
PRKACA guide 3: TTTCACTGAAAGGGAGAGAG
Single cells were sorted into 96-well plates by FACS according to GFP fluorescence and individual clones were expanded for testing. Clones were first assayed for loss of protein expression of RIIα, RIIβ and Cα by Western blotting. Clones that had low or undetectable levels of these proteins were further checked for mutations by purification of genomic DNA and PCR of the appropriate region. PCR products were cloned into pCRBluntII (ThermoFisher) and 8-12 individual colonies were chosen for plasmid DNA mini-prep and sequencing.

Negative Stain Electron Microscopy

MBP-AKAP79-6xHis, 6xHis-PKA catalytic (C) subunit, and RIIα–6xHis regulatory subunit were produced in BL21(DE3) pLysS *E. coli* cells (ThermoFisher). Expression was induced with 0.5 mM IPTG for 4 h at 37 ˚C. Proteins were purified using immobilized metal affinity chromatography (IMAC), followed by size-exclusion chromatography (SEC) using a Superdex 200 10/300 GL column (GE Healthcare) with SEC buffer (20 mM HEPES, pH 7.5, 200 mM NaCl). Individual subunits were incubated at 4˚ C overnight with a molar ratio of 1:2.5:3 AKAP79:RII:C in order to promote formation of a complete complex. These assemblies were subjected to SEC again to isolate fully-formed AKAP79:2RII:2C complexes, which were then prepared for EM using the GraFix method (33). Dilute samples were applied to carbon coated grids and negative-stained with uranyl formate. Grids were imaged on a Tecnai T12 TEM at 0.7-1.5 micron defocus ranges using the Leginon package (34). The initial set of ~14,000 particles were autopicked using DoGPicker (35). Particles were refined through multiple rounds to a set of 3513 particles and iteratively sorted by reference-free 2D classification using RELION (5) until high-quality class averages were obtained. Particles were low-pass filtered to 20 Å to improve contrast.

In vitro Pull-down Assays for AKAP79-PKA Complexes

6xHis-PKA catalytic (C) subunit, RIIα-6xHis regulatory subunit and GST-AKAP79 (amino acids 297-427) were produced in BL21(DE3)pLysS *E. coli* cells (Novagen). Expression was induced with 0.5 mM IPTG for 18 h at 18°C. Proteins were purified using either immobilized metal affinity chromatography (IMAC) or glutathione sepharose, followed by size exclusion chromatography using a HiLoad 16/600 Superdex 200 column (GE Healthcare) equilibrated in 50 mM Tris/HCl, pH 7.4, 100 mM NaCl, 10 % (v/v) glycerol and 1 mM DTT. Purified GST-AKAP79$^{297-417}$ containing a 3C protease cleavage site was incubated on ice for 3 hours with glutathione Sepharose beads, washed five times in binding buffer (50 mM Tris pH 7.4, 0.1M NaCl) and resuspended at a final concentration of ~2μM AKAP79$^{297-417}$. C-subunit (~16 μM final concentration) and RIIα-subunits (~4 μM final concentration) were incubated with beads in the presence or absence of the indicated concentration of cAMP for 20 mins at 30°C with constant agitation. The supernatant was then removed, and after three washes in binding buffer, complexes were eluted from the beads by incubation with 250 ng of 3C protease for 30 minutes at 30°C. Proteins were analysed by SDS-PAGE on a 12% gel. The percentage of C-subunit bound to the AKAP:RIIa complexes was calculated by densitometry using Image J software, and plotted as a function of cAMP concentration.

Pentamer Formation and Analysis by Ion Mobilization Native Mass Spectrometry

Formation of the pentamer (and associated sub-complexes) was achieved by incubating AKAP79$^{297-427}$ (0.75 μM), RIIα (1.88 μM) and C-subunit (2.25 μM) (molar ratio 1:2.5:3

with a final volume of 100 µl) in 20 mM HEPES, 100 mM NaCl overnight at 4 °C. No additional cAMP was included. The sample was buffer exchanged into 100 mM NH_4OAc, 1 mM Tris (pH 7.5) prior to native nESI-MS using a Synapt G2-S*i* instrument (Waters). The sprayer voltage was ~1.5 kV, sampling cone was kept at 150 V, source temperature was 80°C, with the instrument operating in mobility mode. Argon pressure in the ion trap and transfer tube was set to $3*10^{-2}$ mbar. The He cell was 4.5 mbar. Pressure in the ion mobility tube, filled with nitrogen, was 2.8 mbar. Bias voltage for transfer from the ion trap to ion mobility cell was adjusted to 50 V.

Ion Mobilization Native Mass Spectrometry

AKAP binding studies were conducted using a Waters Synapt G2-S*i* instrument. PKA C-subunit (1.5 µM), RIIα (1.5 µM) and $AKAP79^{297-417}$ (3 µM) were incubated for 20 min at 37°C in 100 mM NH_4OAc and analyzed using borosilicate emitters (Thermo Scientific ES 387). cAMP-dependent experiments were performed on a Thermo Exactive Plus EMR instrument. PKA C-subunit (2.5 µM) and RIIα (2.5 µM) were incubated at room temperature for 10 min in 200 mM NH_4OAc, with cAMP being added to the final stated concentration and incubated again for 10 min prior to nano-Electrospray analysis using borosilicate emitters.

High Resolution Analysis with the Exactive EMR Orbitrap

To determine the stoichiometry of cAMP binding to RII:C complexes, the Exactive EMR Orbitrap (ThermoScientific) was operated at a resolution of 17500 (FWHM at m/z 200). The sprayer voltage was ~1.5 kV. Source ionization was maintained at 200 V.

Data Deconvolution

To assist in MS data interpretation, the native mass spectra were processed using UniDec (36), allowing molecular ions to be assigned and for the generation of the zero charge (deconvoluted) mass spectra.

Cell Lysis, Immunoprecipitation and Immunoblotting

HEK293 or U2OS cells were transiently transfected (TransIT LT1; Mirus) with vectors encoding various proteins according to figures and legends. For most experiments, after 40–48 hr and prior to harvesting, the cells were serum starved in DMEM for 1 hr at 37°C. The cells were then treated with vehicle or drug according to the following conditions. For figure 2, cells were preincubated for 5 min at 37°C with DMSO or PDE inhibitors, followed by addition of 1 µM isoproterenol for a further 5 min at 37°C. Cells were harvested in lysis buffer (25 mM HEPES, pH 7.4, 150 mM NaCl, 1 mM EDTA, 1 mM EGTA, 20 mM NaF, 2% glycerol, 0.3% Triton X-100) containing 100 nM okadaic acid and protease inhibitors. AKAP79 or AKAP18γ complexes were immunoprecipitated with anti-GFP rabbit IgG (Invitrogen) and protein A agarose for 2 hr at 4°C. Beads were washed 4 × 1 ml in lysis buffer. Proteins were separated on 4–12% NuPAGE gradient

gels (ThermoFisher) and transferred to nitrocellulose membranes. Primary antibodies used include: PKA catalytic subunit mAb (BD Biosciences clone 5B), 1:1000; RIIα mAb (BD clone 40), 1:2000; GFP mAb (Santa Cruz Biotechnology sc-9996), 1:2000; phospho-PKA substrates rabbit mAb (Cell Signaling Technology (100G7E); 1:1000) were incubated with membranes overnight at 4°C in TBST/Blotto. The membranes were washed extensively in TBST, incubated with HRP-labeled secondary antibodies (Jackson Immunoresearch), washed as before and developed using ECL (ThermoFisher) on an Alpha Innotech MultiImage III with FluoroChem Q software. For re-probing, membranes were stripped with 1X Re-Blot Plus Strong (Millipore) for 15 minutes and then re-blocked in Blotto before incubation with primary antibodies again.

Proximity Ligation Assays

Cells were cultured on 12-18 mm poly-L-lysine coated glass coverslips. After 24-30 hours, cells were starved for 1 hour and then stimulated with appropriate agonists (see figures). Cells were fixed in PHEM (60 mM PIPES, 25 mM HEPES, 10 mM EGTA, 2 mM $MgCl_2$, pH 6.9) containing 4% paraformaldehyde (PFA) (Electron Microscopy Sciences) for 20 minutes. Cells were washed extensively in PBS followed by permeabilization in PBS/0.5% Triton X-100 for 10 minutes. After several PBS washes, cells were processed for PLA according to (37) and manufacturer's instructions using the Orange detection kit with anti-mouse and anti-rabbit reagents (OLink/Sigma-Aldrich). Mouse anti-RIIα mAb (BD clone 40) and rabbit anti-PKAc (SCBT sc-903) were used to detect PKA holoenzymes. Z-stacks of fluorescent images were collected using a Leica DMI6000B inverted microscope with a spinning disk confocal head (Yokagawa) and a CoolSnap HQ camera (Photometrics) controlled by MetaMorph 7.6.4 (Molecular Devices). Maximum intensity projections were quantified for puncta number using Fiji/ImageJ. Images were smoothened and a duplicate image was created for use as a mask. The duplicate file was thresholded to capture as many puncta as possible without significant blending of densely packed signal. The binary mask was then used to measure selected regions from the original image. Total cell number per field of view was counted as DAPI-stained nuclei. Intensity profiles of raw images were produced in MetaMorph.

Live-cell FRET Imaging

HEK293 or U2OS cells were cultured on 35-mm glass coverslip dishes (MatTek Corporation) or 4-well glass bottom coverglass (ibidi). Cells were transiently transfected with cDNAs encoding different reporters alone, or together with either R2C2 fusion constructs or cDNAs encoding individual RII and C subunits. 24-48 hr after transfection, the cells were starved for 1 hour and then imaged in HEPES-Buffered Saline Solution (HBSS; 116 mM NaCl, 20 mM HEPES, 11 mM Glucose, 5 mM $NaHCO_3$, 4.7 mM KCl, 2.5 mM $CaCl_2$, 1.2 mM $MgSO_4$, 1.2 mM KH_2PO_4, pH 7.4). All imaging was performed at ambient temperature (25 - 28^{o}C). Cells were stimulated as indicated in individual figures. Fluorescence emission was acquired using a DMI6000B inverted microscope (Leica), an

EL6000 component (fluorescent light source, filter wheel, ultrafast shutter; Leica) and a CoolSnap HQ camera (Photometrics), all controlled by MetaMorph 7.6.4 (Molecular Devices). Dual-emission images were obtained simultaneously through a DualView image splitter (Photometrics) with S470/30 and S535/30 emission filters and 505 dcxr dichroic mirror (Chroma). Exposure times were 100-500 ms. FRET changes within regions of interest were calculated as the ratio of measured fluorescent intensities from two channels (M_{donor}, $M_{indirectAcceptor}$) after subtraction of background signal. FRET ratio (YFP/CFP) changes were normalized to the average FRET ratio value before stimulation.

Bad Phosphorylation by Immunoblot

U2OS$^{R2A/R2B/CA}$ cells were plated in 6-well dishes and co-transfected with constructs encoding WT or M120A PKA-R2C2 fusion proteins and pEBG-mBad (Cell Signaling Technology; 100-250 ng/well). After ~36 hours, cells were starved for 1 hour in serum free DMEM-H (ThermoFisher). Cells were preincubated for 5 min at 37°C with DMSO or 2 μM 1-NM-PP1, followed by addition of 1 μM iso for a further 5 min at 37°C. Cells were lysed in 25 mM HEPES, pH 7.4, 150 mM NaCl, 1 mM EDTA, 1 mM EGTA, 20 mM NaF, 2% glycerol, 1% Triton X-100, 0.5% deoxycholate plus 100 nM okadaic acid and protease inhibitors. After cell debris removal by centrifugation, protein content of lysates was quantified using the BCA assay (ThermoFisher) in a 96-well plate. Equivalent amounts of total lysate (12-15 μg/lane) was separated on Bolt gradient gels (ThermoFisher) and transferred to nitrocellulose. Membranes were incubated with primary antibodies overnight at 4°C in TBST/Blotto. Prior to re-probing, membranes were stripped with 1X Re-Blot Plus Strong (Millipore) for 15 minutes and then re-blocked in Blotto. The following antibodies were used: phospho-Bad ser155 (Santa Cruz Biotechnology sc-101641), 1:1000; PKA-C mAb (BD clone 5B), 1:1000; GST (Santa Santa Cruz Biotechnology sc-459), 1:1000; GST-HRP (GenScript), 1:1000); GAPDH (Santa Cruz Biotechnology sc-25778), 1:1000. The membranes were washed extensively in TBST, incubated with HRP-labeled secondary antibodies (Jackson Immunoresearch), washed as before and developed using ECL (ThermoFisher) on an Alpha Innotech MultiImage III with FluoroChem Q software. Quantification using densitometry of pSer155 Bad signal was performed using Fiji/ImageJ and normalized to corresponding GST immunoblot signal (for total Bad).

Apoptosis Assay using Fluorescent DEVD Substrate

U2OS$^{R2A/R2B/CA}$ cells were transfected with constructs encoding WT or M120A PKA-R2C2 fusion proteins. Cells were re-plated onto poly-L-lysine coated 8-well chambered coverslips (ibidi) and incubated overnight in vehicle or 50μM etoposide (SCBT). Isoproterenol (1 μM) and the long-acting β-agonist formoterol (1 μM) (an attempt to keep β-AR-PKA signaling high during the time course of the overnight treatment) were also added to appropriate wells. After 16 hours, CellEvent™ Caspase-3/7 Green Detection Reagent (ThermoFisher) was added to cells at a final concentration of 2 μM for 1 hour at

37°C. Cells were fixed by direct addition of PFA (16%, Electron Microscopy Sciences) to 4% for 5 minutes. Media was then replaced with PBS containing 4% PFA for another 10 minutes. Cells were washed extensively in PBS, permeabilized for 10 minutes in PBS containing 0.5% Triton X-100 and 0.2% BSA and then washed several times in PBS. Cells were incubated with DAPI for 20 minutes and stored in PBS. For imaging, PBS was replaced with Vectashield (Vector Labs). Images were acquired on our Leica spinning-disk confocal microscope as described above.

Cell Growth Assay

U2OS$^{R2A/R2B/CA/CB}$ (R2C2-M120A stable, Cβ KO) cells were created as described above, using a sgRNA targeting PRKACB (sequence: 5'-CATGGCATAATACTGTTCAG-3'). Several clones with interruptions of the PRKACB gene were expanded and subjected to cell growth assays using the CellTiter 96® AQ_{ueous} One Solution cell proliferation assay (Promega, Madison, WI). Cells were plated in a 96-well plate in triplicate at 1000 cells per well in 100 μl. After 24 hours, 20 μl assay solution was added to each well and cells were grown another 3 hours at 37°C, 5% CO_2. Absorbance at 490 nm was read on a POLARstar Omega plate reader (BMG Labtech). Counts were background subtracted using wells containing only growth media.

Figure S1

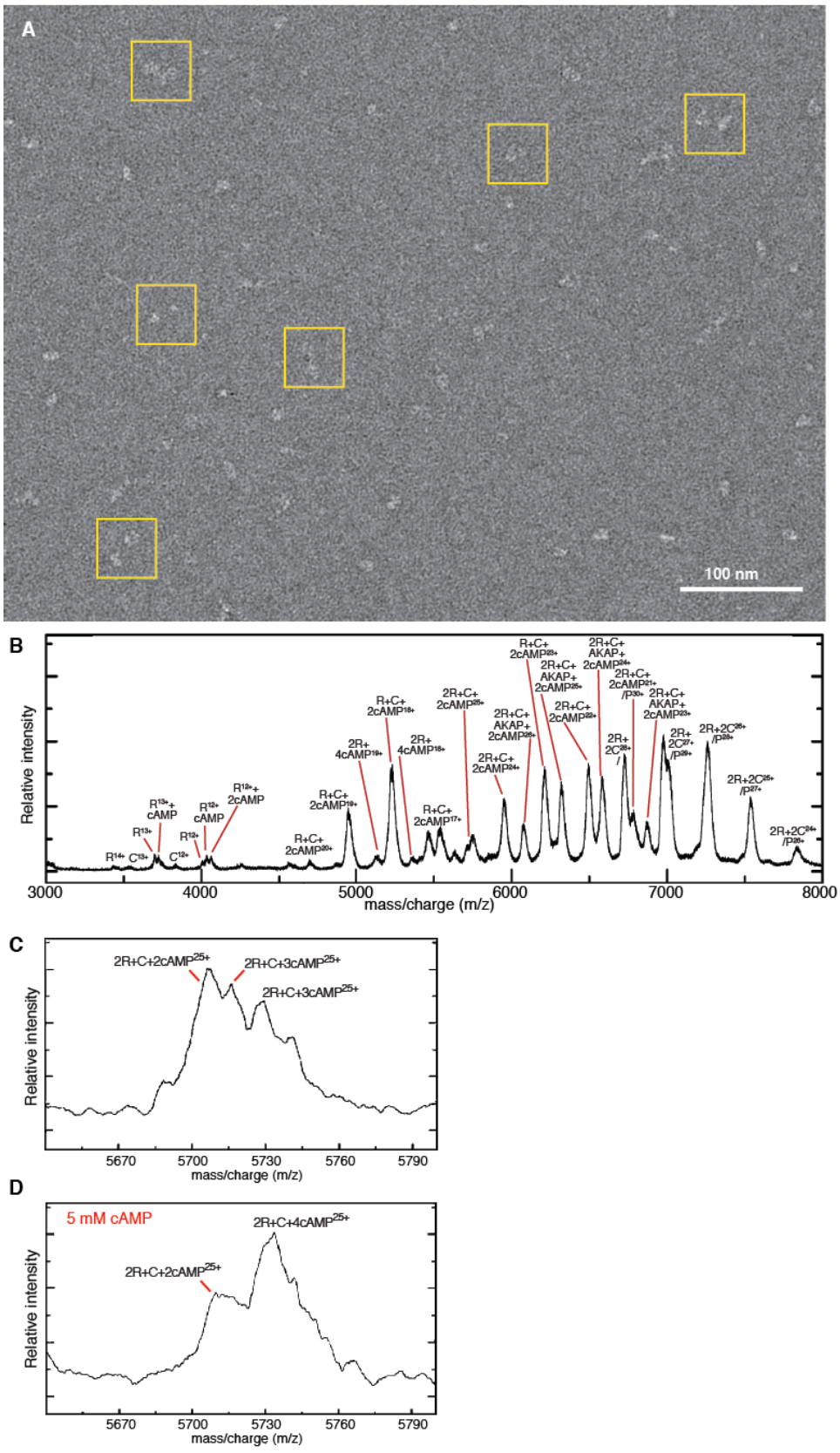
A
100 nm
B
Relative intensity
mass/charge (m/z)
3000
4000
5000
6000
7000
8000
C
2R+C+2cAMP25+
2R+C+3cAMP25+
2R+C+3cAMP25+
Relative intensity
mass/charge (m/z)
5670
5700
5730
5760
5790
D
5 mM cAMP
2R+C+4cAMP25+
2R+C+2cAMP25+
Relative intensity
mass/charge (m/z)
5670
5700
5730
5760
5790

Fig. S1.

Additional data related to figure 1. **(A)** Raw EM micrograph of AKAP79-PKA holoenzyme complexes, low-pass filtered to 20 Å. Purified proteins were assembled into complexes and processed by the GraFix method (43). Dilute samples were applied to carbon coated grids and negative-stained with uranyl formate. Grids were imaged on a Tecnai T12 TEM at 0.7-1.5 micron defocus ranges. Representative particles picked for further analysis are boxed (yellow squares). **(B)** Native nESI mass spectrum of RII+C+AKAP$^{297\text{-}427}$ complexes. Indicated are the charge states of each of the observed and annotated molecular ions (see associated tables S1 and S2). Data were acquired on the Synapt G2-S*i* (Waters). **(C)** Native nESI mass spectrum of RII+C complexes without additional cAMP. The 25+ charge state of the 2RII:C:**n**cAMP complexes are presented (see associated table S3). Data were acquired on the Exactive™ Plus EMR Orbitrap (ThermoScientific). **(D)** Native nESI mass spectrum of RII+C complexes with additional cAMP (5 µM; RII:C:cAMP ratio of 1:1:2). The 25+ charge state of the 2RII:C:**n**cAMP complexes are presented (see associated table S3). Data were acquired on the Exactive™ Plus EMR Orbitrap (ThermoScientific).

Figure S2

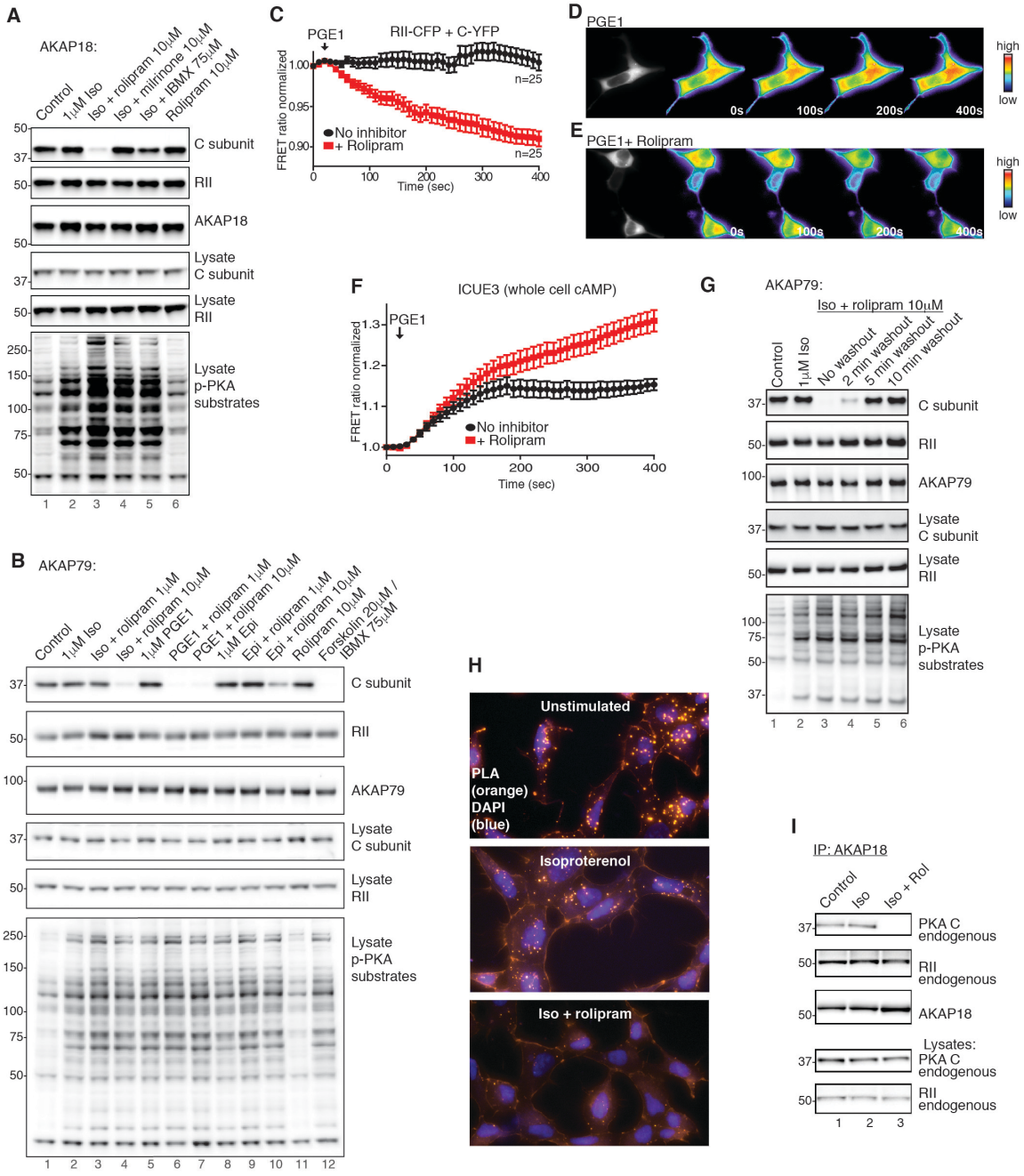

Fig. S2

Additional data related to figure 2. *Anchored PKA holoenzymes remain associated during submaximal cAMP pulses and can re-form quickly upon removal of supraphysiological stimuli.* **(A)** HEK293 cells expressing AKAP18γ-GFP and RIIa-V5 were stimulated for 5 minutes with 1 μM isoproterenol alone or after 5-minute pre-incubation with PDE inhibitors as indicated. AKAP18γ was immunoprecipitated, and immune complexes and lysates were probed for associated PKA subunits by Western

blotting. Detection of phosphorylated PKA substrates was used to confirm activation of PKA signaling. **(B)** HEK293 cells expressing AKAP79-GFP and RIIα-V5 were stimulated for 5 minutes with indicated compounds alone or after 5-minute pre-incubation with PDE inhibitors as above. Forskolin/IBMX treatment was for 20 minutes. AKAP79 was immunoprecipitated and immune complexes and lysates were probed for associated PKA subunits by Western blotting. Detection of phosphorylated PKA substrates was used to confirm activation of PKA signaling. **(C)** FRET recordings in HEK293 cells expressing the paired RII-CFP/PKAc-YFP biosensor upon PGE_1 stimulation in the presence (red) or absence (black) of rolipram. **(D)** Representative images from PGE_1 treated cells. **(E)** Representative images from PGE1 + rolipram treated cells. **(F)** FRET recordings in HEK293 cells expressing the ICUE3 cAMP biosensor upon PGE_1 stimulation in the presence (red) or absence (black) of rolipram. **(G)** HEK293 cells expressing AKAP79-GFP and RIIα-V5 were stimulated for 5 minutes with 1 μM isoproterenol or were stimulated with iso + rolipram followed by a washout period of different lengths in which drug was removed and replaced with fresh serum-free DMEM. AKAP79 was then immunoprecipitated, and immune complexes and lysates were probed for associated PKA subunits. Detection of phosphorylated PKA substrates was used to confirm activation of PKA signaling. **(H)** HEK293 cells on glass coverslips were stimulated as described above and then fixed in 4% PFA for proximity ligation assays. Cells were processed for detection of the interaction between RII and C with the Orange PLA detection kit (Sigma-Aldrich) and co-stained for DAPI to detect nuclei. **(I)** HEK293 cells expressing AKAP18γ-GFP were stimulated for 5 minutes with 1 μM isoproterenol alone or after 5-minute pre-incubation with rolipram (10 μM). AKAP18γ was immunoprecipitated, and immune complexes and lysates were probed for associated PKA subunits by Western blotting.

Figure S3

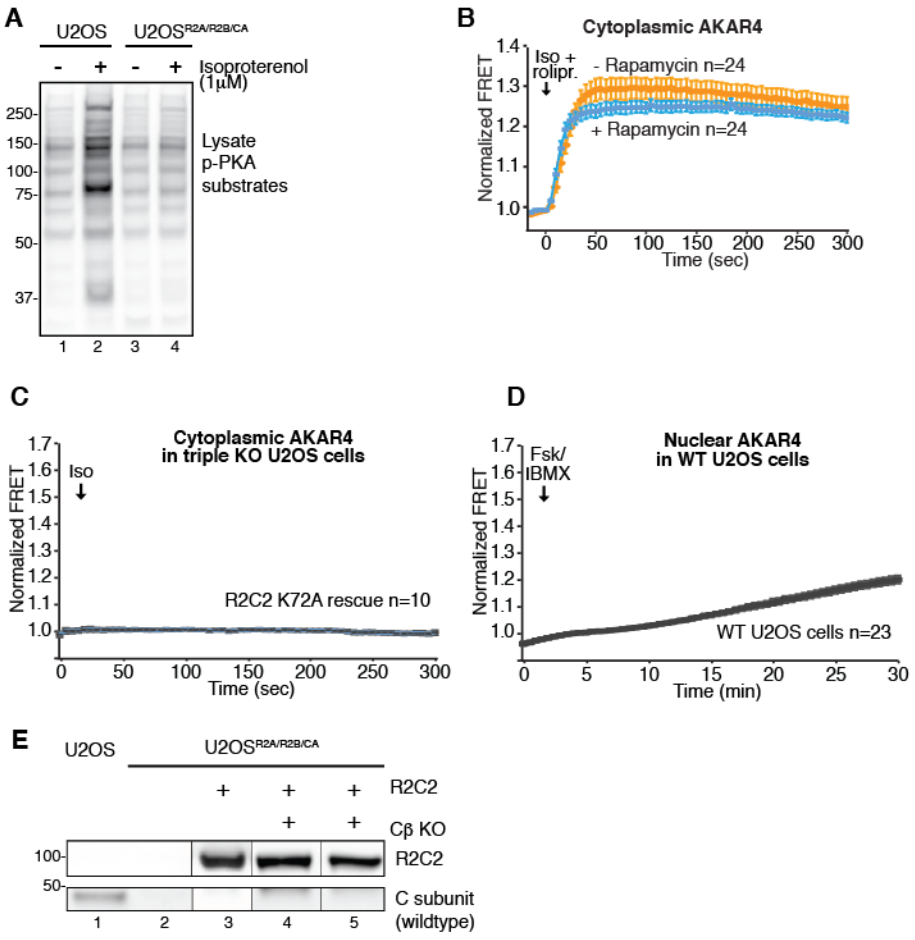

Fig. S3

Additional data related to figure 3. **(A)** Immunoblotting using phospho-PKA substrates antibodies of cell lysates from wild-type U2OS and U2OS$^{R2A/R2B/CA}$ cells after treatment with isoproterenol (1 μM, 5 min). **(B)** Cytoplasmic AKAR4 FRET recordings in U2OS$^{R2A/R2B/CA}$ cells expressing FKBP-RII and FRB-C in response to stimulation with isoproterenol and PDE4 inhibitor rolipram (1 μM/10 μM), in the absence (orange) or presence (blue) of rapamycin (100 nM). **(C)** AKAR4^{NES} cytoplasmic FRET recordings in Iso-stimulated U2OS$^{R2A/R2B/CA}$ cells expressing "kinase-dead" R2C2 K72A. **(D)** AKAR4^{NLS} nuclear FRET recordings in wild-type U2OS cells in response to forskolin/IBMX treatment. **(E)** Immunoblotting of wild-type U2OS, U2OS$^{R2A/R2B/CA}$, U2OS$^{R2A/R2B/CA}$-R2C2 stable, and two clonal lines of U2OS$^{R2A/R2B/CA/CB}$-R2C2 stable (Cβ KO) cells with antibodies against PKA C-subunit. These blots were assembled from two different experiments to demonstrate stable expression of the R2C2 fusion protein.

Figure S4

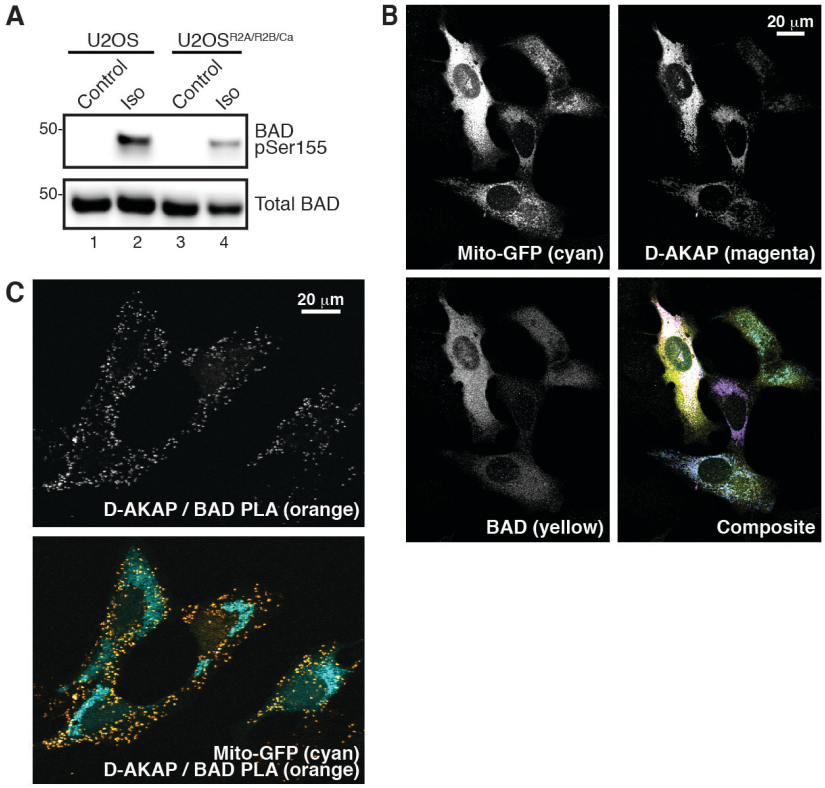

Fig. S4

Additional data related to figure 4. **(A)** Wild-type U2OS and U2OS$^{R2A/R2B/CA}$ were transfected with a plasmid encoding GST-BAD. Cells were treated with isoproterenol (1 μM) or vehicle for 5 minutes. Immunoblot detecting BAD pSer155 and total BAD (GST). **(B)** U2OS$^{R2A/R2B/CA}$ transiently expressing mitochondrially-targeted GFP, D-AKAP-1 and GST-BAD were fixed, stained and imaged using confocal microscopy. **(C)** U2OS$^{R2A/R2B/CA}$ transiently expressing mitochondrially-targeted GFP, D-AKAP-1 and GST-BAD were fixed, processed for proximity ligation and imaged using confocal microscopy. Fluorescence is shown in grayscale except for composite images.

Table S1: Theoretical and observed *m/z* values for each of the observed complexes of RII, C, AKAP79$^{297-427}$ with or without cAMP as measured by native MS. Data were acquired on the Synapt G2-S*i* (Waters).

Complex	Charge state	[a] *m/z* theoretical	*m/z* observed	[b] delta
C	12	3834.9	3834.4	-0.5
	13	3540.0	3535.1	-4.9
RII	12	4006.3	4004.7	-1.6
	13	3698.2	3699.4	1.2
	14	3434.1	3433.4	-0.7
RII:cAMP	12	4033.8	4034.0	0.2
	13	3723.6	3723.9	0.3
RII:2cAMP	12	4061.2	4061.4	0.2
	13	3748.9	3747.9	-1.0
2RII:4cAMP	18	5414.6	5419.3	4.7
	19	5129.7	5130.7	1.0
RII:C	17	5534.6	5540.6	6.0
	18	5227.2	5228.5	1.3
	19	4952.1	4951.7	-0.4
	20	4704.6	4704.2	-0.4
2RII:C:2cAMP	22	6491.6	6497.4	5.8
	23	6209.4	6213.7	4.3
	24	5950.7	5952.5	1.8
	25	5712.7	5717.7	5.0
2RII:2C	24	7840.3	7834.7	-5.6
	25	7526.7	7538.3	11.6
	26	7237.2	7260.4	23.2
	27	6969.2	6977.7	8.5
2RII:C:AKAP:2cAMP	23	6868.4	6872.0	3.6
	24	6582.2	6582.5	0.3
	25	6319.0	6320.3	1.3
	26	6076.0	6077.7	1.7
2RII:2C:AKAP (P)	26	7820.2	7834.7	14.5
	27	7530.6	7538.3	7.7
	28	7261.6	7260.4	-1.2
	29	7011.3	7006.1	-5.2
	30	6777.6	6782.0	4.4

[a] Theoretical masses (and *m/z* values) of the complexes were calculated using the native experimental mass data for the individual subunits under the same experimental conditions.

[b] Difference between theoretical and observed values arise due to incomplete desolvation and adducts of Na^+ that are typical of these types of native mass spectrometry analyses.

Table S2: Theoretical and experimentally computed masses (Da) of each of the observed complexes of RII, C, AKAP79$^{297-427}$ with or without cAMP following native MS (Supplementary Table 1; Fig 1). Data were acquired on the Synapt G2-S*i* (Waters).

Complex	[a]Theoretical mass (Da)	Experimental mass (Da)	[b]Delta mass (Da)
R:C	94,071	94,000	71
2R:C:2cAMP	142,793	142,600	193
2R:C:AKAP:2cAMP	157,949	157,800	149
2R:2C	188,142	188,100	42
2R:2C:AKAP	203,298	203,200	98

[a] Theoretical masses of the complexes were calculated using the native experimental mass data for the individual subunits under the same experimental conditions.

[b] It should be noted that the difference between theoretical and observed values arise largely due to incomplete desolvation and adducts of Na^+ that are typical of these types of native mass spectrometry analyses. Consideration should also be given to the multiple phosphorylated forms of the catalytic subunit C, given that an average of 7 (5 – 10) phosphate molecules are typically observed for heterologously expressed catalytic enzyme (Ref. 10).

Table S3: Theoretical and observed *m/z* values for the 25+ charge state of the 2RII:C:ncAMP complexes, without or with additional cAMP (5 µM; RII:C:cAMP ratio of 1:1:2), as measured by native MS. Data were acquired on the Exactive™ Plus EMR Orbitrap (ThermoScientific).

RII:C:cAMP Ratio	Complex	Charge state	[a] *m/z* theoretical	*m/z* observed	[b] delta
1:1:0	**2RII:C:2cAMP**	25	5706.1	5706.6	0.5
	2RII:C:3cAMP	25	5719.3	5715.8	-3.5
	2RII:C:4cAMP	25	5732.4	5728.4	-4.0
1:1:2	**2RII:C:2cAMP**	25	5706.1	5712.8	6.7
	2RII:C:4cAMP	25	5732.4	5732.8	0.4

[a] Theoretical masses (and m/z values) of the complexes were calculated using the native experimental mass data for the individual subunits under the same experimental conditions.

[b] Difference between theoretical and observed values arise due to incomplete desolvation and adducts of Na^+ that are typical of these types of native mass spectrometry analyses.

References and Notes

1. D. A. Walsh, J. P. Perkins, E. G. Krebs, An adenosine 3',5'-monophosphate-dependent protein kinase from rabbit skeletal muscle. *J. Biol. Chem.* **243**, 3763–3765 (1968). Medline

2. R. L. Potter, S. S. Taylor, Relationships between structural domains and function in the regulatory subunit of cAMP-dependent protein kinases I and II from porcine skeletal muscle. *J. Biol. Chem.* **254**, 2413–2418 (1979). Medline

3. D. R. Knighton, J. H. Zheng, L. F. Ten Eyck, V. A. Ashford, N. H. Xuong, S. S. Taylor, J. M. Sowadski, Crystal structure of the catalytic subunit of cyclic adenosine monophosphate-dependent protein kinase. *Science* **253**, 407–414 (1991). doi:10.1126/science.1862342 Medline

4. L. K. Langeberg, J. D. Scott, Signalling scaffolds and local organization of cellular behaviour. *Nat. Rev. Mol. Cell Biol.* **16**, 232–244 (2015). doi:10.1038/nrm3966 Medline

5. S. H. Scheres, RELION: Implementation of a Bayesian approach to cryo-EM structure determination. *J. Struct. Biol.* **180**, 519–530 (2012). doi:10.1016/j.jsb.2012.09.006 Medline

6. F. D. Smith, S. L. Reichow, J. L. Esseltine, D. Shi, L. K. Langeberg, J. D. Scott, T. Gonen, Intrinsic disorder within an AKAP-protein kinase A complex guides local substrate phosphorylation. *eLife* **2**, e01319 (2013). doi:10.7554/eLife.01319 Medline

7. A. J. Heck, Native mass spectrometry: A bridge between interactomics and structural biology. *Nat. Methods* **5**, 927–933 (2008). doi:10.1038/nmeth.1265 Medline

8. M. G. Gold, F. Stengel, P. J. Nygren, C. R. Weisbrod, J. E. Bruce, C. V. Robinson, D. Barford, J. D. Scott, Architecture and dynamics of an A-kinase anchoring protein 79 (AKAP79) signaling complex. *Proc. Natl. Acad. Sci. U.S.A.* **108**, 6426–6431 (2011). doi:10.1073/pnas.1014400108 Medline

9. D. P. Byrne, M. Vonderach, S. Ferries, P. J. Brownridge, C. E. Eyers, P. A. Eyers, cAMP-dependent protein kinase (PKA) complexes probed by complementary differential scanning fluorimetry and ion mobility-mass spectrometry. *Biochem. J.* **473**, 3159–3175 (2016). doi:10.1042/BCJ20160648 Medline

10. M. Zaccolo, T. Pozzan, Discrete microdomains with high concentration of cAMP in stimulated rat neonatal cardiac myocytes. *Science* **295**, 1711–1715 (2002). doi:10.1126/science.1069982 Medline

11. P. J. Silver, Biochemical aspects of inhibition of cardiovascular low (K_m) cyclic adenosine monophosphate phosphodiesterase. *Am. J. Cardiol.* **63**, 2A–8A (1989). doi:10.1016/0002-9149(89)90384-6 Medline

12. S. L. Jin, T. Bushnik, L. Lan, M. Conti, Subcellular localization of rolipram-sensitive, cAMP-specific phosphodiesterases. Differential targeting and activation of the splicing variants derived from the PDE4D gene. *J. Biol. Chem.* **273**, 19672–19678 (1998). doi:10.1074/jbc.273.31.19672 Medline

13. J. Zhang, R. E. Campbell, A. Y. Ting, R. Y. Tsien, Creating new fluorescent probes for cell biology. *Nat. Rev. Mol. Cell Biol.* **3**, 906–918 (2002). doi:10.1038/nrm976 Medline

14. L. M. DiPilato, J. Zhang, The role of membrane microdomains in shaping beta2-adrenergic receptor-mediated cAMP dynamics. *Mol. Biosyst.* **5**, 832–837 (2009). doi:10.1039/b823243a Medline

15. O. Söderberg, K. J. Leuchowius, M. Kamali-Moghaddam, M. Jarvius, S. Gustafsdottir, E. Schallmeiner, M. Gullberg, J. Jarvius, U. Landegren, Proximity ligation: A specific and versatile tool for the proteomic era. *Genet. Eng. (N.Y.)* **28**, 85–93 (2007). Medline

16. K. J. Herbst, M. D. Allen, J. Zhang, Spatiotemporally regulated protein kinase A activity is a critical regulator of growth factor-stimulated extracellular signal-regulated kinase signaling in PC12 cells. *Mol. Cell. Biol.* **31**, 4063–4075 (2011). doi:10.1128/MCB.05459-11 Medline

17. S. S. Taylor, R. Ilouz, P. Zhang, A. P. Kornev, Assembly of allosteric macromolecular switches: Lessons from PKA. *Nat. Rev. Mol. Cell Biol.* **13**, 646–658 (2012). doi:10.1038/nrm3432 Medline

18. D. J. Morgan, M. Weisenhaus, S. Shum, T. Su, R. Zheng, C. Zhang, K. M. Shokat, B. Hille, D. F. Babcock, G. S. McKnight, Tissue-specific PKA inhibition using a chemical genetic approach and its application to studies on sperm capacitation. *Proc. Natl. Acad. Sci. U.S.A.* **105**, 20740–20745 (2008). doi:10.1073/pnas.0810971105 Medline

19. M. S. Lopez, J. I. Kliegman, K. M. Shokat, The logic and design of analog-sensitive kinases and their small molecule inhibitors. *Methods Enzymol.* **548**, 189–213 (2014). doi:10.1016/B978-0-12-397918-6.00008-2 Medline

20. H. Harada, B. Becknell, M. Wilm, M. Mann, L. J. Huang, S. S. Taylor, J. D. Scott, S. J. Korsmeyer, Phosphorylation and inactivation of BAD by mitochondria-anchored protein kinase A. *Mol. Cell* **3**, 413–422 (1999). doi:10.1016/S1097-2765(00)80469-4 Medline

21. J. M. Lizcano, N. Morrice, P. Cohen, Regulation of BAD by cAMP-dependent protein kinase is mediated via phosphorylation of a novel site, Ser155. *Biochem. J.* **349**, 547–557 (2000). doi:10.1042/bj3490547 Medline

22. Y. Tan, M. R. Demeter, H. Ruan, M. J. Comb, BAD Ser-155 phosphorylation regulates BAD/Bcl-XL interaction and cell survival. *J. Biol. Chem.* **275**, 25865–25869 (2000). doi:10.1074/jbc.M004199200 Medline

23. K. Virdee, P. A. Parone, A. M. Tolkovsky, Phosphorylation of the pro-apoptotic protein BAD on serine 155, a novel site, contributes to cell survival. *Curr. Biol.* **10**, R883 (2000). doi:10.1016/S0960-9822(00)00843-5 Medline

24. E. H. Cheng, T. V. Sheiko, J. K. Fisher, W. J. Craigen, S. J. Korsmeyer, VDAC2 inhibits BAK activation and mitochondrial apoptosis. *Science* **301**, 513–517 (2003). doi:10.1126/science.1083995 Medline

25. G. Manning, D. B. Whyte, R. Martinez, T. Hunter, S. Sudarsanam, The protein kinase complement of the human genome. *Science* **298**, 1912–1934 (2002). doi:10.1126/science.1075762 Medline

26. J. D. Scott, C. W. Dessauer, K. Taskén, Creating order from chaos: Cellular regulation by kinase anchoring. *Annu. Rev. Pharmacol. Toxicol.* **53**, 187–210 (2013). doi:10.1146/annurev-pharmtox-011112-140204 Medline

27. N. Hoshi, L. K. Langeberg, C. M. Gould, A. C. Newton, J. D. Scott, Interaction with AKAP79 modifies the cellular pharmacology of PKC. *Mol. Cell* **37**, 541–550 (2010). doi:10.1016/j.molcel.2010.01.014 Medline

28. N. Hoshi, L. K. Langeberg, J. D. Scott, Distinct enzyme combinations in AKAP signalling complexes permit functional diversity. *Nat. Cell Biol.* **7**, 1066–1073 (2005). doi:10.1038/ncb1315 Medline

29. H. Hehnly, D. Canton, P. Bucko, L. K. Langeberg, L. Ogier, I. Gelman, L. F. Santana, L. Wordeman, J. D. Scott, A mitotic kinase scaffold depleted in testicular seminomas impacts spindle orientation in germ line stem cells. *eLife* **4**, e09384 (2015). doi:10.7554/eLife.09384 Medline

30. B. Lygren, C. R. Carlson, K. Santamaria, V. Lissandron, T. McSorley, J. Litzenberg, D. Lorenz, B. Wiesner, W. Rosenthal, M. Zaccolo, K. Taskén, E. Klussmann, AKAP complex regulates Ca2+ re-uptake into heart sarcoplasmic reticulum. *EMBO Rep.* **8**, 1061–1067 (2007). doi:10.1038/sj.embor.7401081 Medline

31. J. C. Chrivia, R. P. S. Kwok, N. Lamb, M. Hagiwara, M. R. Montminy, R. H. Goodman, Phosphorylated CREB binds specifically to the nuclear protein CBP. *Nature* **365**, 855–859 (1993). doi:10.1038/365855a0 Medline

32. M. Hagiwara, P. Brindle, A. Harootunian, R. Armstrong, J. Rivier, W. Vale, R. Tsien, M. R. Montminy, Coupling of hormonal stimulation and transcription via the cyclic AMP-responsive factor CREB is rate limited by nuclear entry of protein kinase A. *Mol. Cell. Biol.* **13**, 4852–4859 (1993). doi:10.1128/MCB.13.8.4852 Medline

33. B. Kastner, N. Fischer, M. M. Golas, B. Sander, P. Dube, D. Boehringer, K. Hartmuth, J. Deckert, F. Hauer, E. Wolf, H. Uchtenhagen, H. Urlaub, F. Herzog, J. M. Peters, D. Poerschke, R. Lührmann, H. Stark, GraFix: Sample preparation for single-particle electron cryomicroscopy. *Nat. Methods* **5**, 53–55 (2008). doi:10.1038/nmeth1139 Medline

34. C. Suloway, J. Pulokas, D. Fellmann, A. Cheng, F. Guerra, J. Quispe, S. Stagg, C. S. Potter, B. Carragher, Automated molecular microscopy: The new Leginon system. *J. Struct. Biol.* **151**, 41–60 (2005). doi:10.1016/j.jsb.2005.03.010 Medline

35. N. R. Voss, C. K. Yoshioka, M. Radermacher, C. S. Potter, B. Carragher, DoG Picker and TiltPicker: Software tools to facilitate particle selection in single particle electron microscopy. *J. Struct. Biol.* **166**, 205–213 (2009). doi:10.1016/j.jsb.2009.01.004 Medline

36. M. T. Marty, A. J. Baldwin, E. G. Marklund, G. K. A. Hochberg, J. L. P. Benesch, C. V. Robinson, Bayesian deconvolution of mass and ion mobility spectra: From binary interactions to polydisperse ensembles. *Anal. Chem.* **87**, 4370–4376 (2015). doi:10.1021/acs.analchem.5b00140 Medline

37. O. Söderberg, K.-J. Leuchowius, M. Gullberg, M. Jarvius, I. Weibrecht, L.-G. Larsson, U. Landegren, Characterizing proteins and their interactions in cells and tissues using the in situ proximity ligation assay. *Methods* **45**, 227–232 (2008). doi:10.1016/j.ymeth.2008.06.014 Medline